Design and Construction of the LEIR Extraction Septum

J. Borburgh, M. Crescenti, M. Hourican, T. Masson

***Abstract*—The Low Energy Ion Ring (LEIR) is part of the LHC injector chain for ions. The LEIR extraction will use a pulsed magnetic septum, clamped around a metallic vacuum chamber which plays an important role in separating the high vacuum in the LEIR ring (dynamic pressure ~ 10^{-12} mbar) from that in the transfer line to the PS, where the vacuum requirements are less stringent. The major technical challenges and novel solutions related to the design of this magnet will be presented.**

Index Terms—**Accelerator magnets, Particle beam extraction, Vacuum technology, Mechanical engineering.**

I. Introduction

THE Low Energy Ion Ring (LEIR) allows to accumulate long pulses from Linac 3 into high brilliance ion bunches for LHC by means of multi-turn injection, electron cooling and accumulation [1]. The LEIR extraction septum (ER.SMH40) is a pulsed magnetic septum to limit the power dissipation and hence the cooling requirements and complexity of the magnet coil. Because of the very stringent vacuum requirements in the LEIR ring, with dynamic vacua in the 10^{-12} mbar range, and more so since the magnet yoke for this application needs to be laminated, the magnet will be clamped around a metallic vacuum chamber. The vacuum chamber will be part of the magnet and play a role in separating the required vacuum in the LEIR ring from the less stringent vacuum requirements for the transfer line towards the PS ring. Also the vacuum chamber helps to reduce the fringe field of the magnet. Table 1 shows the main parameters of the extraction septum. Its design is based on a beam rigidity of 4.8 T.m, corresponding to an energy of 72 MeV/nucleon for lead ions. The septum is installed in the LEIR extraction line to the PS (see figure 1). It is a pulsed single turn magnet with a thin-wall stainless steel vacuum chamber in the magnet gap. This vacuum chamber, with a circular cross section, is segmented to follow the beam trajectory. To allow the vacuum chambers to be baked out at 300°C or to provide access to the magnet coil for maintenance, the septum conductor can be unbolted from the yoke and rear conductors, and subsequently the magnet, which is mounted on slides, can be pulled away from the vacuum chamber.

TABLE I
MAIN PARAMETERS OF THE LEIR EXTRACTION SEPTUM ER.SMH40

Deflection angle	130	mrad
Integrated magnetic field (∫B.dl)	0.624	T.m
Gap field	0.738	T
Integrated fringe field	<0.7	mT.m
Gap width between conductors	90	mm
Gap height	48	mm
Magnet length	900	mm
Magnetic equivalent length	845	mm
Septum conductor thickness	4.5 Cu + 0.5 stainless steel	mm
Effective septum thickness as seen by the beam	10	mm
Number of conductor turns	1	
Inside diameter of magnet vacuum chamber	44	mm
Magnet vacuum chamber wall thickness	1	mm
Peak current	28.2	kA
RMS current	750	A
Half sine pulse width	Approx. 5	ms
Flat top duration	>400	μs
Magnet inductance	2.5	μH
Magnet resistance	0.14	mΩ

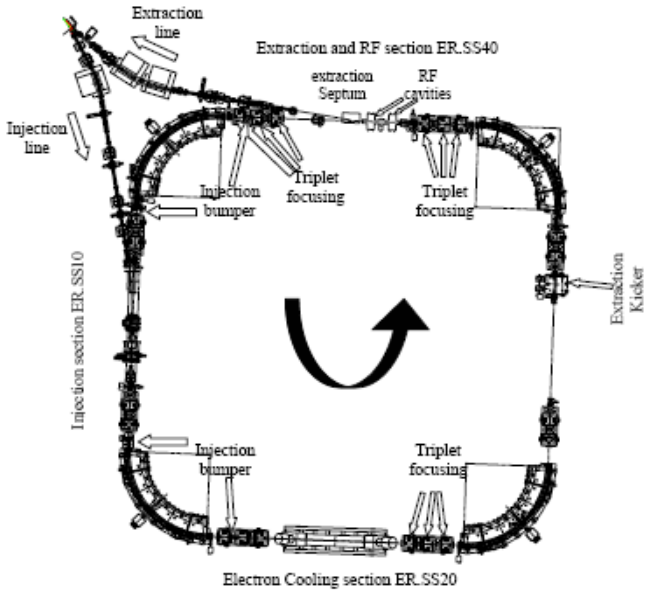

Fig. 1. The extraction septum as located in the LEIR ring

Manuscript received September 18th, 2005.

J. Borburgh, M. Hourican and T. Masson are with CERN, 1211 Geneva 23, Switzerland (e-mail: jan.borburgh@cern.ch).

M. Crescenti is with the TERA foundation, Novara, Italy (e-mail: Massimo.Crescenti@cern.ch).

II. MAGNETIC CIRCUIT DESIGN

A. 2D steady state design

The design of the magnet allows for dismantling of the magnet horizontally, away from the installed vacuum chambers. In particular the septum conductor is tapered at 45° on the top and bottom sides to locate the conductor in place when being pressed from the outside. The location of the cooling channels and the height of the septum conductor compared to the gap height are optimised to obtain a field homogeneity in the gap of ±0.5 % of the nominal field. The coloured region in the magnet gap in figure 2 shows the area with this field uniformity for a steady state calculation as performed with the finite element program FLUX2D.

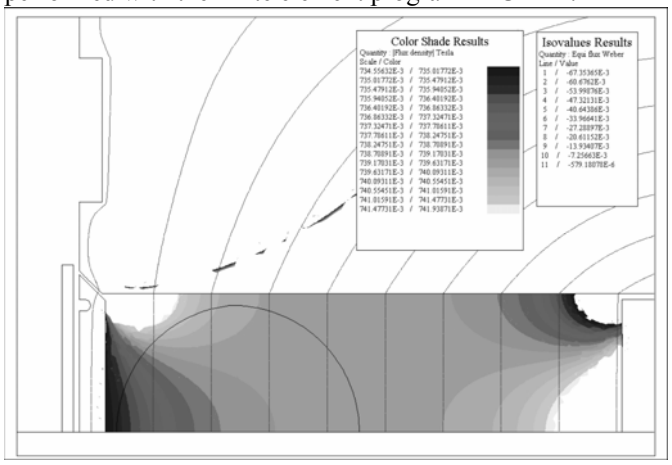

Fig. 2. 2D Field calculation with Flux2D of the magnet gap field. The field in the coloured area is within ±0.5% of the nominal field.

Outside the magnet a mumetal screen of 2 mm thickness (consisting of a 50-50 % Ferro-Nickel alloy) is required to reduce the fringe field sufficiently. To stay within the 10 mm constraint for the apparent septum thickness as seen by the beam, this screen actually forms part of the orbiting beam vacuum chamber. The fringe field values predicted by the finite element simulation using FLUX2D are shown in figure 3, and show that the fringe field should be less than 1 ‰ of the gap field.

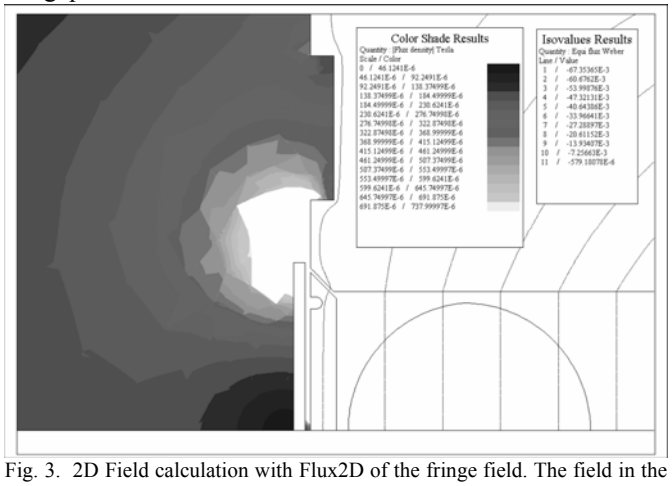

Fig. 3. 2D Field calculation with Flux2D of the fringe field. The field in the coloured area is lower than 1mT.

B. 3D steady state design

The magnetic length of the septum was determined using the Vector Fields Tosca / Opera 3D finite element software. The steel used for the yoke is silicon steel. The endplates in the finite element model were chosen to be of Armco. The model indicates that the magnet as designed and as being manufactured will have a magnetic length of 845 mm.

C. Transient behaviour

Since the magnet is outside the vacuum chamber for vacuum reasons, and pulsed to limit the power dissipation, and hence the cooling requirements, it is essential to verify that the magnetic field will penetrate the stainless steel vacuum chamber.

It can be shown [2] [3] that for a round vacuum chamber in a changing dipole field, the field in the centre of the vacuum chamber is delayed by τ_r and that the eddy current time constant is τ_0 where τ_0 and τ_r are defined as follows:

$$\tau_0 = \mu_0 \sigma d \tfrac{r}{2} \quad (1)$$

$$\tau_r = \tau_0 (1 + \tfrac{1}{3}(\pi r/h)^2) \quad (2)$$

where d is the vacuum chamber wall thickness, r the radius of the vacuum chamber, h the magnet gap height and σ the electrical conductivity of the vacuum chamber material. In the present application the vacuum chamber has a 1 mm wall thickness, and a 44 mm internal diameter and the magnet gap is 48 mm. The field delay is 25 μs and the time constant is 15 μs.

The field error due to the eddy currents in the vacuum chamber wall (f_s) and including the image currents ($f_i(z)$) can be expressed as follows:

$$f_s = -\frac{\tau_0}{dB/dt} \quad (3)$$

$$f_i(z) = f_s\left(1 + \left(\frac{r}{z}\right)^2 - \left(\pi \frac{r}{h \sinh\left(\frac{\pi z}{h}\right)}\right)^2\right) \quad (4)$$

where, z = x+iy describes the position (x,y) inside the vacuum chamber with respect to its centre in complex coordinates. Assuming the applied dipole field varies with a half sine pulse width of 3.3 ms with superimposed 3rd harmonic to create a flat top, the field error due to the eddy currents would by less than ±0.0002 T during 600 μs as shown in figure 4. The extraction time is 700 ns, and the influence of the eddy currents can be neglected in this time scale. In reality the magnet will be powered with a 5 ms half sine pulse with a 3rd harmonic correction and an additional active filter which assures a real flat top ($<10^{-4}$) for more than 400 μs, and therefore the eddy currents will disturb the field even less.

Due to the fact that the septum is pulsed, the yoke will be constructed of laminated steel. The skin depth of steel can be calculated as follows:

$$\delta = \sqrt{\frac{2}{2\pi f .\sigma .\mu_0 \mu_r}} \quad (5)$$

where δ is the skin depth, f the equivalent frequency at which the magnet is pulsed and μ_r the relative magnetic permeability. For steel and at f=150 Hz, and μ_r=5000, the skin depth is 0.57 mm. Consequently, standard magnetic 3 % silicon steel of 0.35 mm thickness is used for the laminations.

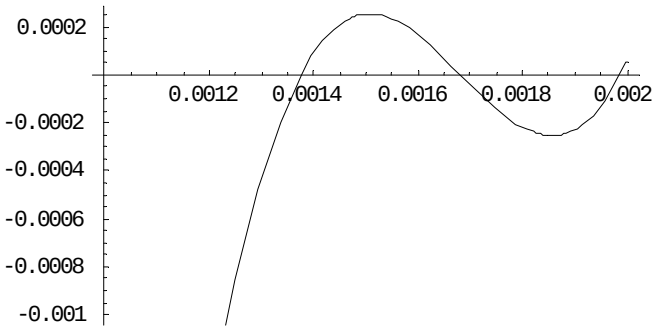

Fig. 4. The field error calculated for the centre of the vacuum chamber due to the eddy currents. The magnetic field is a 150 Hz equivalent half sine pulse with a third harmonic. It can be observed that between 0.0013 s and 0.002 s the field error is less than 0.0002T.

D. Cooling

Despite the modest specific rms current density in the septum conductor of 5.1 A mm^{-2}, cooling channels have been inserted in the coil to stabilise the temperature and hence the electrical resistance as seen by the power supply. The location of the cooling channels in the septum conductor has been chosen such that together with the effect of the tapering of the edges of the conductor the best global current uniformity is achieved in both top and bottom of the conductor. This will help to decrease the fringe field and improve the field uniformity in the gap. One hydraulic circuit will cool the septum conductor, and two independent circuits will provide cooling for each half rear conductor. The flow will be approximately 1 $l.min^{-1}$ for each cooling circuit.

III. MECHANICAL DESIGN OF THE MAGNET AND COIL

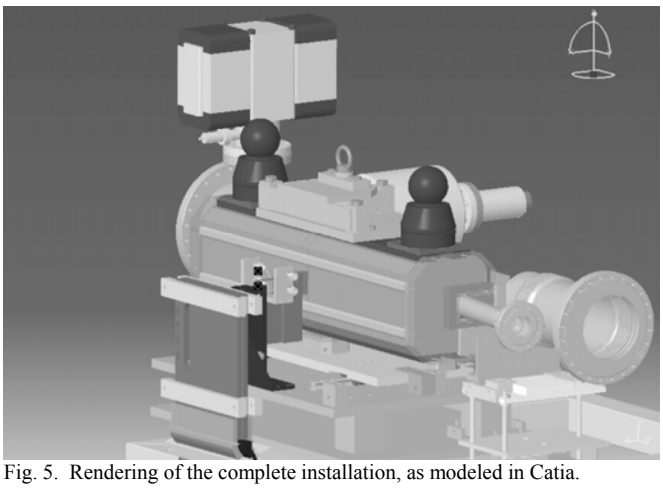

Fig. 5. Rendering of the complete installation, as modeled in Catia.

A. Yoke design and assembly

The yoke design has been finalised and is currently in the fabrication stage. The laminations will be held together by longitudinal bars which will be welded to the laminations following stacking and alignment in an assembly jig. The coil rear conductor will be inserted in the yoke followed by installation of the magnet yoke around the vacuum chamber (see figure 5). The septum conductor will then be inserted parallel with the magnet and mumetal side wall and screwed to the crossover coil pieces. The coil is retained in position by the clamps which fix the rigid section of the vacuum chamber wall to the magnet yoke (see figure 6).

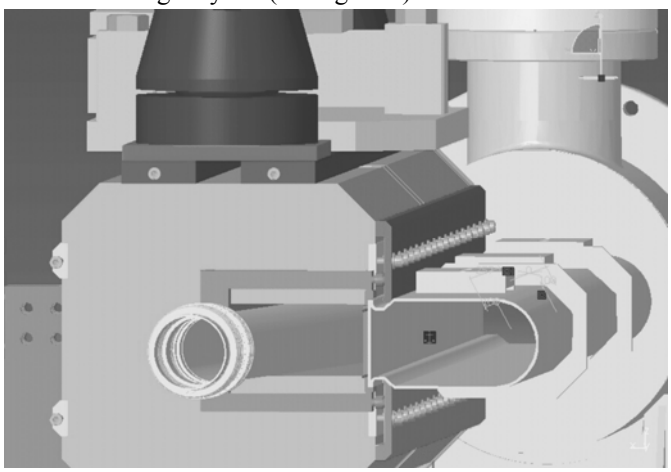

Fig. 6. Magnet and ejection vacuum chamber with exit flanges removed.

B. Coil Design

The coil has been manufactured in individual part, consisting of the septum blade, rear conductor and cross over pieces. Individual cooling circuits have been embedded in the septum blade and rear conductor (see figure 7). The coil is insulated from the yoke by a 0.2 mm thick layer of ceramic (Al_2O_3) which is deposited both on the coil and the yoke using a plasma deposition technique. A 0.1 mm Kapton® sheet is inserted between the coil and yoke to further improve the insulation properties.

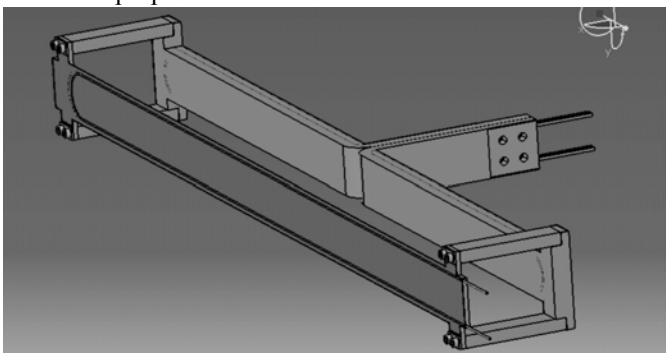

Fig. 7. The coil assembly as modeled in Catia.

The main advantage of this coil design is the possibility to easily change the septum blade in the event of a failure. The magnet does not require removal from the vacuum chamber to facilitate this operation. During bakeout the septum blade is removed and the magnet, which is mounted on roller slides, can be easily withdrawn from the vacuum chamber. The

magnet is powered through a 12:1 pulse transformer which is mounted below the magnet assembly in order to occupy the minimum of space.

IV. VACUUM CHAMBER DESIGN AND CONSTRUCTION

The complicated geometry (see figures 8 and 9) and design constraints of the vacuum chamber required extensive studies in order to develop the mechanically stable, bakeable, and magnetically acceptable assembly. In order to produce the correct magnetic field for ejection the stainless steel tube for the ejection line had to be optimised for its thickness and mechanical stability. A tube with wall thickness 1 mm, incorporating a ceramic insulating transition piece was welded between the entry and exit flanges. The vacuum chamber for the circulating beam has to fulfil multiple roles. Apart from the use as a pure vacuum chamber (imposing vacuum related constraints on its design), it also retains the magnet coil in the yoke using a system of clamps. Consequently its design should also cope with 8.8×10^3 N of electromechanical force

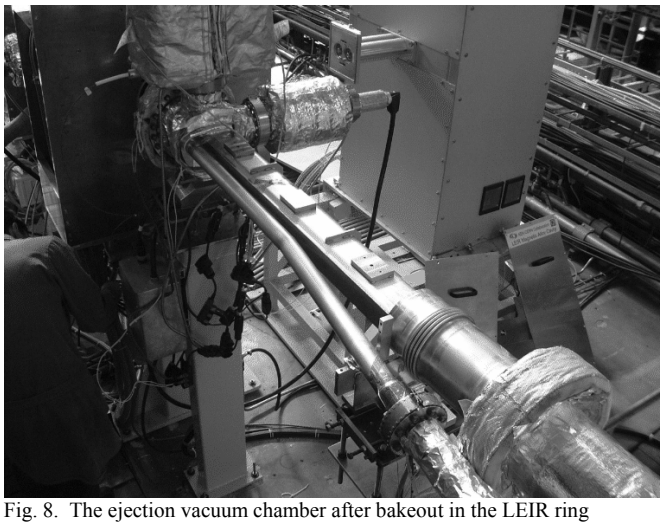

Fig. 8. The ejection vacuum chamber after bakeout in the LEIR ring

from the adjacent septum conductor when the magnet is pulsed. As mentioned earlier, it also serves as a magnetic screen (limiting the choice of the materials for the orbiting beam vacuum chamber wall to 2 mm mumetal). Finally it contributes to the vacuum pumping due a NEG coating deposited on the inner surface of the tube.

The manufacture of the chamber with its complicated form involved many different production techniques in a predetermined sequence of operations. The mumetal side wall was electron beam welded to the main tube. The flanges were CNC-machined according to the final dimensions of the welded tube prior to final assembly and the ejection tube was assembled in two individual lengths to follow as close as possible the beam trajectory. The ceramic piece prevents induced electrical currents in the vacuum chamber which would counteract the magnetic field when the magnet is pulsed, like a short cut secondary winding of a transformer. Two bellows assemblies have been fitted to each tube to allow for thermal expansion during the 300 °C bakeout and to cater for any minor distortions due to the multiple welding procedures. After final assembly, the complete chamber has been NEG coated with approximately 1.5 µm of titanium-vanadium-zirconium alloy thus increasing the effective pumping capacity in the sector.

Pumping is provided for by means of a titanium sublimation pump and an ion pump mounted on a pumping port at the

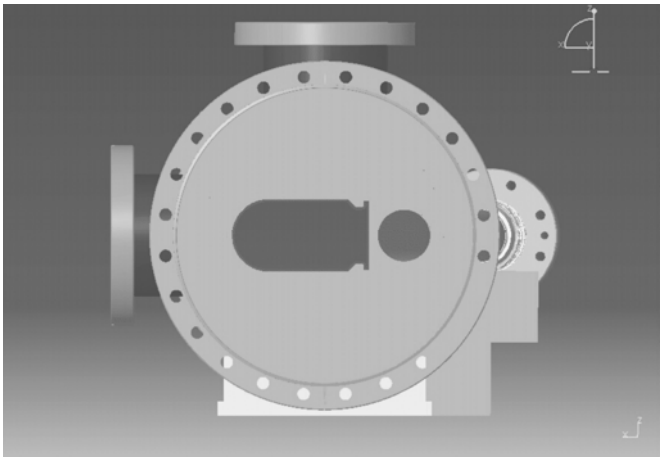

Fig. 9. The ejection vacuum chamber cross section

entry to the vacuum chamber. The NEG coating applied to the vacuum chamber increases the effective pumping speed and also reduces the secondary emission rates from the chamber walls. Penning and Pirani gauges are also fitted to the chamber. The nominal dynamic pressure is expected to be in the 10^{-12} mbar range following bakeout.

V. STATUS AND OUTLOOK

The vacuum chamber is installed in the LEIR ring, and bakeout is underway. The septum coil has been brazed prior to receiving the ceramic insulation layer. The magnet yoke will be constructed of 0.35 mm thick 3 % silicon steel laminations welded to stainless steel bars, although a glued yoke would have been preferred. However, due to the difficulties in the procurement of the raw material the welded solution had to be retained. In autumn this year the magnet assembly will take place, and magnetic measurements will have to confirm the predicted magnetic length as seen by the beam inside the stainless steel vacuum chamber. Installation of the magnet inside the LEIR ring, around its vacuum chamber, is schedule for the end 2005.

ACKNOWLEDGMENT

The realisation of this magnet is the collaborative effort of many people from various CERN groups and departments. The authors would like to thank them all for their co-operation.

REFERENCES

[1] Eds. M. Benedikt, P. Collier, V. Mertens, J. Poole. LHC Design Report: Volume III, The LHC Injector Chain. CERN. Geneva. December 2004.
[2] W M. Chanel and Ch. Carli, private communication..
[3] F.Schaeff. Field distortions produced by eddy currents in metallic vacuum chambers of the PSB 800 MeV C.O. deflectors. CERN. Internal Note SI/Note MAE/69-11. July 1969.